High-performance Reactive Magnesium Cement Incorporating Hollow Natural Fiber and Silica Sand

Bo Wu[1,*], and *Jishen* Qiu[1]

[1]Department of Civil and Environmental Engineering, Hong Kong University of Science and Technology, Clear Water Bay, Hong Kong, China

Abstract. Global warming caused by CO_2 emissions makes reactive magnesium cement (RMC) increasingly attractive due to its ability to sequester CO_2, however, the diffusion of CO_2 in RMC is severely limited by the dense hydrated magnesium carbonates (HMCs) formed on the outer layer. This work utilizes hollow natural fiber (e.g., sisal fiber) to facilitate the diffusion of CO_2 into the deep part of the RMC specimen. Combining with adding silica sand as a filling agent, the mechanical strength can be enhanced from 42.4 MPa of the control group to 92.6 MPa of the specimen with 2 vol.% sisal fiber, this is attributed to that the addition of sisal fiber significantly enhances the carbonation depth. FTIR and XPS results further prove that the addition of 2 vol.% or more sisal fiber can improve the carbonation degree by over 200%, leading to a sharp reduction of CO_2 emission from 37 kg/(m^3·MPa) of the control group to 12.1 kg/(m^3·MPa) of the specimen with 2 vol.% sisal fiber. Therefore, adding hollow natural fiber and silica sand to RMC can be a promising approach to make RMC stronger and more sustainable.

1 Introduction

Increasing demand for Portland cement (PC) contributes to about 10% of total anthropogenic CO_2 emissions, threatening the global climate and ecosystem [1]. This adverse impact on the environment has stimulated the research for sustainable binders with a low carbon footprint. Among emerging low-carbon binders, reactive magnesia cement (RMC) has gradually been accepted as a sustainable alternative to PC [2-4] due to: 1) lower calcination temperature (i.e., 700 - 1000°C for RMC vs. 1450°C for PC); and 2) the ability to sequester ambient CO_2. In addition to being a carbon reservoir, the RMC has also demonstrated prominent autogenous healing performance, the matrix cracks can be completely healed after several wetting-air cycles due to the abundance of Mg^{2+}, which can easily react with dissolved CO_2 to form hydrated magnesium carbonates (HMCs) [3, 5]. Furthermore, MgO-based expansive agents were also added to PC against shrinkage-induced cracks or to enhance the healing efficiency [6, 7].

The reactive MgO can firstly hydrate in water to form brucite followed by carbonation to form different HMCs [2, 8]. The formation of HCMs accompanies by the solid volume expansion by a factor of 1.8-3.1, which remarkably refines the microstructure and provides comparable or even higher mechanical strength in comparison with PC [9], however, this hinders the further diffusion of CO_2 into the deep part and slows down the mechanical strength development [10, 11].

Hollow natural fiber (HNF) was applied in our previous study to enhance the CO_2 sequestration and mechanical strength of RMC [12], the main mechanism is that the hollow lumens in natural fiber can be the pathway for CO_2 to diffuse into the interior. Even though the incorporation of HNF increases the mechanical strength from 20.9 MPa to 40.3 MPa after 14-day carbonation [12], it was still lower than about 60 MPa of the specimens added with hydration agent (e.g., magnesium acetate) and nucleation seeds (e.g., hydromagnesite) [13]. Furthermore, carbonation of pure RMC may induce cracking due to the formation of expansive HMCs [14], while adding fine aggregate can improve the stability of the matrix [15, 16]. Accordingly, to further enhance the mechanical strength and stability of RMC, sisal fiber and silica sand were introduced into RMC. Mechanical strength, carbonation depth, and carbonation degree of RMC with silica sand and different contents of sisal fiber will be demonstrated in this work.

2 Experimental programs

2.1 Materials

The RMC was acquired from Shanghai Yuanjiang Chemical Co., Ltd, it is composed of 95 wt.% of reactive

* Corresponding author: bwuar@connect.ust.hk

Table 1. Mix proportion used in this work.

Test	MgO	Silica sand	Water	$Na(PO_3)_6$	Sisal fiber (vol.%)	PVA fiber (vol.%)
Compressive	1	0.2	0.58	0.058	0/1/2/4	
	1	0.2	0.58	0.058	4	
Flexural	1	0.2	0.58	0.058	2	1
	1	0.2	0.58	0.058	0	2

MgO and minor impurities like CaO and SiO_2; The sodium hexametaphosphate ($Na(PO_3)_6$) was supplied by Sigma-Aldrich, which is used to modify the rheology of the fresh paste [17]. Long sisal fibers were provided by Zhejiang Rafi Grass Paper Products Co., Ltd, and then cut into 15-mm-long short fibers. The PVA fibers were acquired from Kuraray Ltd with the tensile strength of 1600 MPa, diameter of about 39 μm, and length of 12 mm. The silica sand used in this work has a mean diameter of 150 μm.

2.2 Specimen preparation

Table. 1 shows the mix proportion used in this work. The RMC composites were mixed and cast with the following steps: 1) the $Na(PO_3)_6$ was dissolved into the water, forming the $Na(PO_3)_6$ solution; 2) all the particle ingredients, i.e., MgO and silica sand, were dry-blended in a planetary mixer for three minutes; 3) the $Na(PO_3)_6$ solution was slowly added into the mixer and mixed for three minutes; 4) the fibers were then gradually added and mixed for another three minutes; 5) the fresh paste was cast into 40×40×40 mm^3 cubic molds for compressive test and beam molds with the dimension of 350×60×12 mm^3 for bending test, the specimens were kept in ambient air for 24 hours before demoulding. Then the specimens were moved to an environmental chamber (30 °C, 85% relative humidity, 10% CO_2 concentration) until the date of testing.

2.3 Mechanical tests

Unconfined uniaxial compressive tests were conducted to the cubes with the loading rate of 1 kN/s; for each group three cubes were tested. Three-point bending tests were carried out on an MTS 250KN Universal Testing Machine at a crosshead rate of 0.8 mm/min. Three specimens with a span of 300 mm were tested for each group. Two LVDTs were attached to the midpoint to measure the displacement. The first crack strength (σ_f) is determined by the following equation [18]:

$$\sigma_f = \frac{3F_f L}{2BH^2} \quad (1)$$

where F_f is the end point of linearity in the load-deflection curve, L is the lower fulcrum span (300 mm), B and H are the width and thickness of the specimen, respectively.

2.4 Carbonation detection

After compressive tests, the cubes were cut off in the middle, and the phenolphthalein, which would change to pink if pH>10 [19], was sprayed onto the newly exposed surface as an indicator of carbonation depth. To increase the accuracy, the average depth of the carbonation region was perpendicularly measured from four midpoints of four edges. To quantitatively measure the carbonation degree of specimens at different depths, the central part with dimensions of 20×20×40 mm^3 was taken out from the cubic sample by cutting after 28-day carbonation. The collected prisms were cut into 8 slices with a thickness of 5 mm followed by immersing in isopropanol for 7 days to kill the hydration and carbonation. After which, the slices from the same depth were placed together and grounded. The short sisal fibers in the received powder were further screened out by a sieve with an opening of 0.5 mm. Then the powders were characterized with Fourier transform infrared spectroscopy (FTIR, Bruker Vertex 70 Hyperion 1000) and X-ray photoelectron spectroscopy (XPS, PHI 5600).

Based on the XPS results and mix design, the CO_2 emission (E_C) of different specimens is calculated by the following equation:

$$E_C = \frac{\alpha(P_C - S_C - F_C)}{\sigma} \left(\frac{kg}{m^3 \cdot MPa}\right) \quad (2)$$

where α is the mass fraction of MgO per m^3, P_C and S_C are the CO_2 emissions during MgO production and CO_2 sequestration during curing, respectively. F_C is the carbon fixed in hollow natural fiber, σ is the compressive strength.

3 Results and discussion

3.1 Mechanical performances

Fig. 1a shows the compressive strength of RMC with different contents of sisal fiber. As expected, the incorporation of sisal fiber in RMC induces stronger mechanical strength compared with the control group. At the early stage (e.g., after 3-day curing), all the RMC-based composites present a comparable strength from 35 MPa to 42 MPa, which is due to the early strength of RMC mainly relies on the hydration of MgO [20]. As carbonation progresses, all the specimens demonstrate an increase in strength at different rates and eventually ranked as follows after 28-day curing: RMC_Sisal (2%) > RMC_Sisal (4%) > RMC_Sisal (1%) > RMC_Sisal (0%). Accordingly, 2 vol.% sisal fiber is the optimal dosage to achieve the greatest compressive strength of 92.6 MPa, which is about 2.2 times that of the control group RMC, and also higher than the RMC_Sisal (2%) without silica sand of 58.9 MPa. The maximum strength reported in the previous study was about 70 MPa with the addition of hydration agent and nucleation seeds [13], this work

provides a novel approach involving hollow natural fiber and silica sand to achieve higher strength.

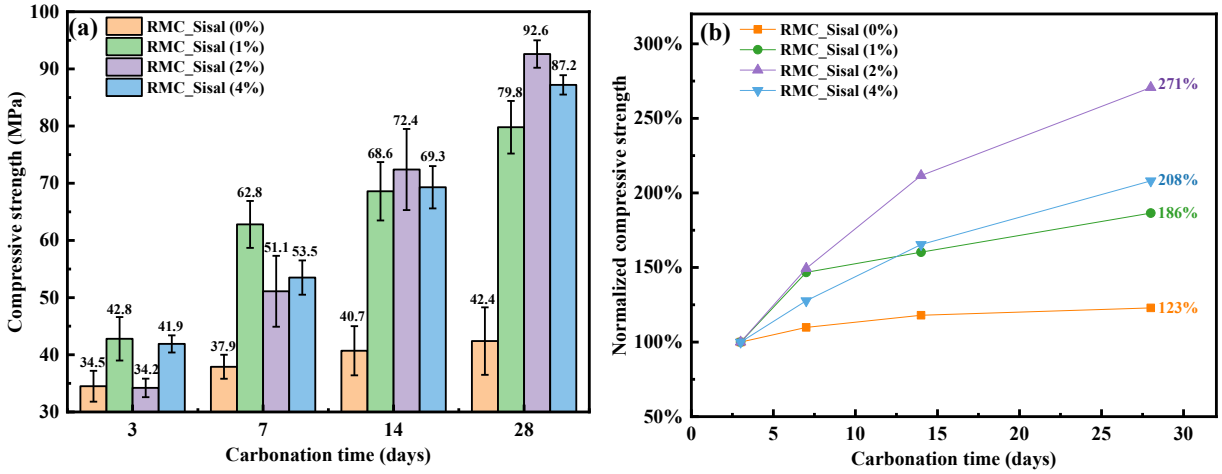

Fig. 1. Compressive strength of (a) RMC with different sisal fibers and (b) its normalized compressive strength.

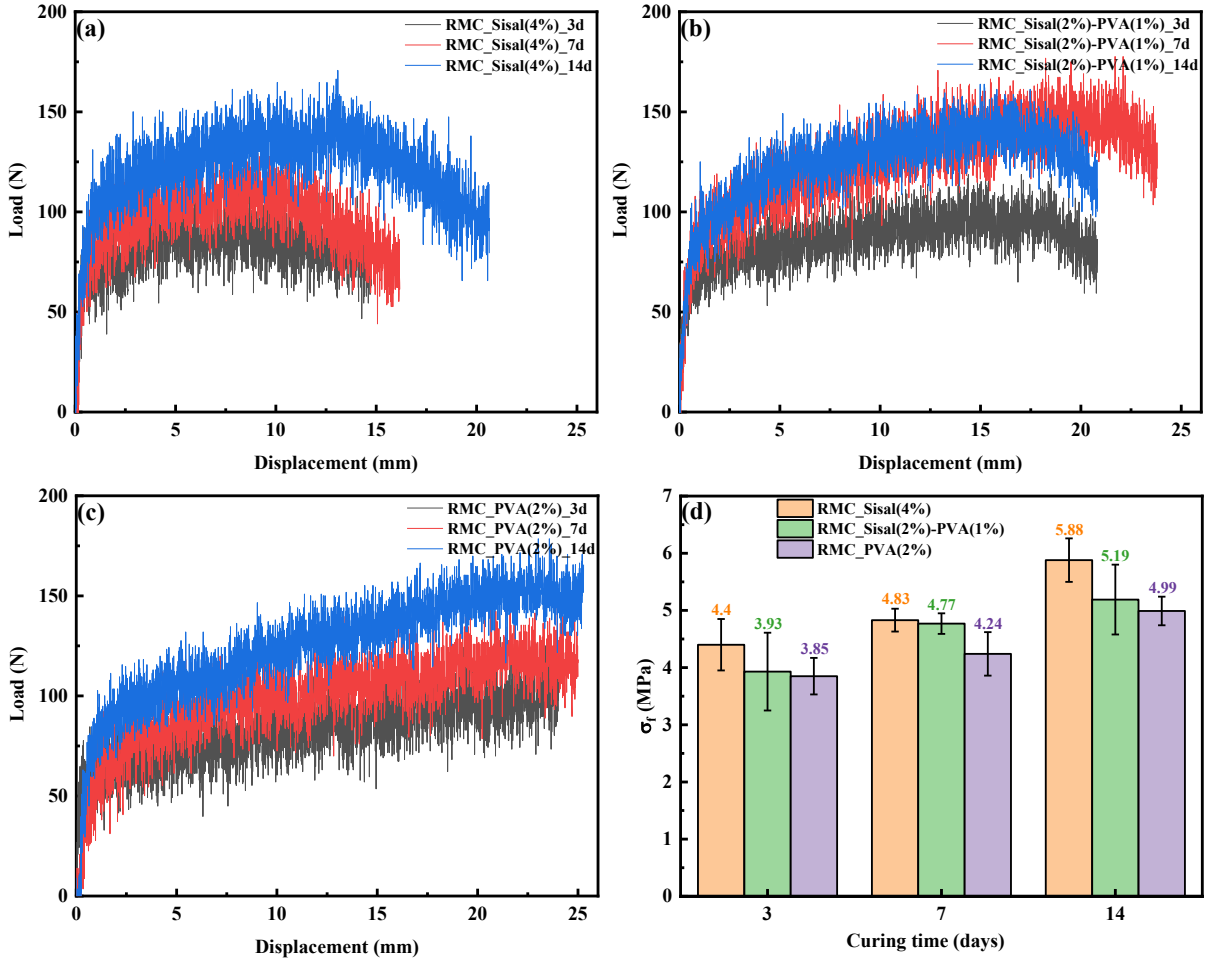

Fig. 2. Representative load-displacement curves of (a) RMC_Sisal (4%), (b) RMC_Sisal (2%)-PVA (1%) and (c) RMC_PVA (2%) after different curing time, (d) is the calculated first crack strength.

Fig. 1b shows the normalized compressive strength relative to the 3-day strength to exhibit the rate of strength development. As it is presented, the RMC incorporated with sisal fiber has a significantly higher strength development rate than the control group. As the mechanical strength of RMC mainly relies on the formation of interconnected HMCs via carbonation [4], the higher development rate in RMC with sisal fiber confirms that the addition of sisal fiber can remarkably facilitate the diffusion of CO_2 in RMC. In contrast, the control group RMC_Sisal (0%) shows the lowest development rate, this can be attributed to the formation of dense HMCs on the outer layer severely inhibits the diffusion of CO_2.

Fig. 2a-c presents the load-displacement curves of RMC_Sisal (4%), RMC_Sisal (2%)-PVA (1%) and

RMC_PVA (2%) after designed carbonation time. All the specimens demonstrate an apparent strain-hardening behavior, and as expected, the substitution of sisal fiber with PVA fiber leads to better ductility. Limited by the measuring range of LVDT, the maximum displacement is about 25 mm in RMC_PVA (2%) and the decline stage of loading was not recorded. The first crack strength of different specimens is depicted in **Fig. 2d**, which also continually grows as carbonation time onwards. The RMC_Sisal (4%) exhibits the maximum first crack strength, and finally reached 5.88 MPa after 14-day curing, which is comparable to the PC-based composites reinforced with natural fiber [21]. Replacement of sisal fiber with PVA fiber results in a decline in first crack strength, this may be due to the lower sisal fiber content reduces the diffusion rate of CO_2 and subsequently the formation of HMCs.

3.2 Carbonation depth and degree

Fig. 3a shows the carbonation frontier of RMC with different contents of sisal fiber after 28-day curing. The phenolphthalein turns pink in the presence of OH^- (e.g., pH > 10), hence no change in color indicates the OH^- was consumed by HCO_3^- derived from the dissolution of CO_2 [19]. As it can be seen, almost all the exposed surfaces of control group RMC_Sisal (0%) are pink, suggesting a negligible carbonation depth, this coincides with the slowest development rate of mechanical strength as shown in **Fig. 1**. Apparently, the incorporation of sisal fiber significantly enhances the carbonation depth, especially for the RMC with 2 vol.% or more sisal fiber, no pink areas were observed. **Fig. 3b** presents the evolution of carbonation depth with curing time. No increase in carbonation depth for RMC_Sisal (0%) can be seen, this proves the formation of HMCs on the outer layer of the specimen severely obstacles the diffusion of CO_2. With the addition of sisal fiber, carbonation depth continuously grows. Noticeably, the growth rate of carbonation depth almost remains unchanged throughout the curing period when the sisal fiber content is 2 vol.% or more, indicating the CO_2 diffusion is unaffected by the carbonation-induced microstructure densification in the presence of sufficient sisal fiber.

Fig. 4a shows the FTIR spectra of samples collected from different depths of RMC with different sisal fiber contents. The peak at 3700 cm^{-1} and ~3450 cm^{-1} belong to the O-H stretching vibration and the shoulder band at 1650 cm^{-1} is assignable to the bending vibration of H_2O [22]. The peak at around 1450 cm^{-1} can be attributed to the antisymmetric stretching vibration of CO_3^{2-} [20], its intensity gradually decays as the content of sisal fiber decreases from 4 vol.% to 1 vol.%, followed by a drop when the fiber content decreases to 0 vol.%, indicating the HMCs proportion shrank with the decrease in sisal fiber content.

Fig. 4b presents the carbon/magnesium molar ratio at different depths. All specimens almost demonstrate a declining trend in C/Mg ratio with the depth, and a sharper decline rate can be seen in RMC_Sisal (0%) and RMC_Sisal (1%). The RMC_Sisal (0%) shows the lowest C/Mg ratio and the value is lower than 0.2 when the depth exceeds 5 mm and finally decreases to about 0.1 at the depth of 15-20 mm, the low carbonation degree in RMC is in agreement with previous studies [11, 13]. With the incorporation of sisal fiber, the C/Mg ratio can be hugely improved, especially for RMC_Sisal (2%) and RMC_Sisal (4%) the C/Mg ratio still exceeds 0.5 even at the depth of 15-20 mm. This dramatic enhancement in carbonation degree corroborates the addition of sisal fiber is a promising approach to enhance the CO_2 sequestration in RMC.

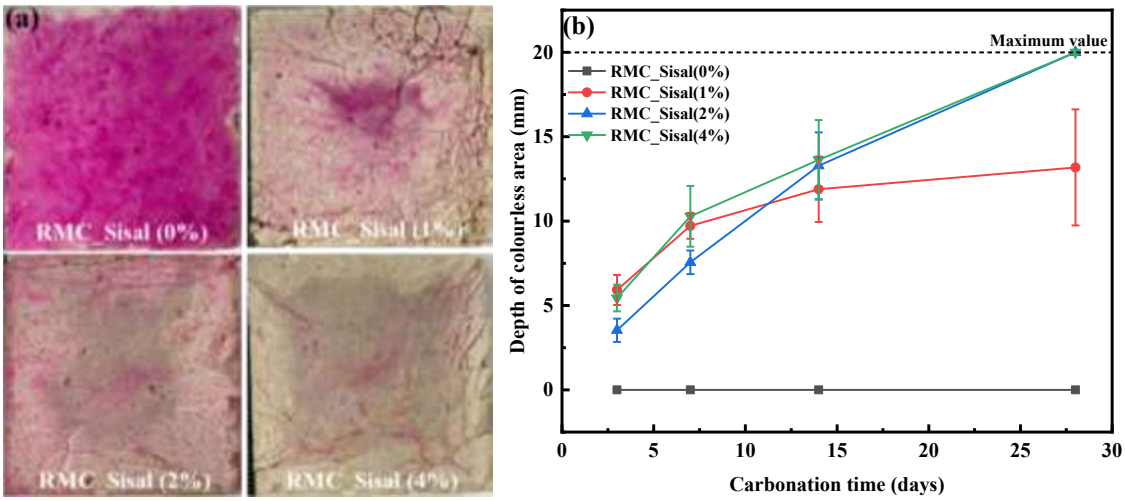

Fig. 3. (a) Carbonation frontier identified by phenolphthalein after 28-day curing; (b) evolution of depth of colourless area with curing time.

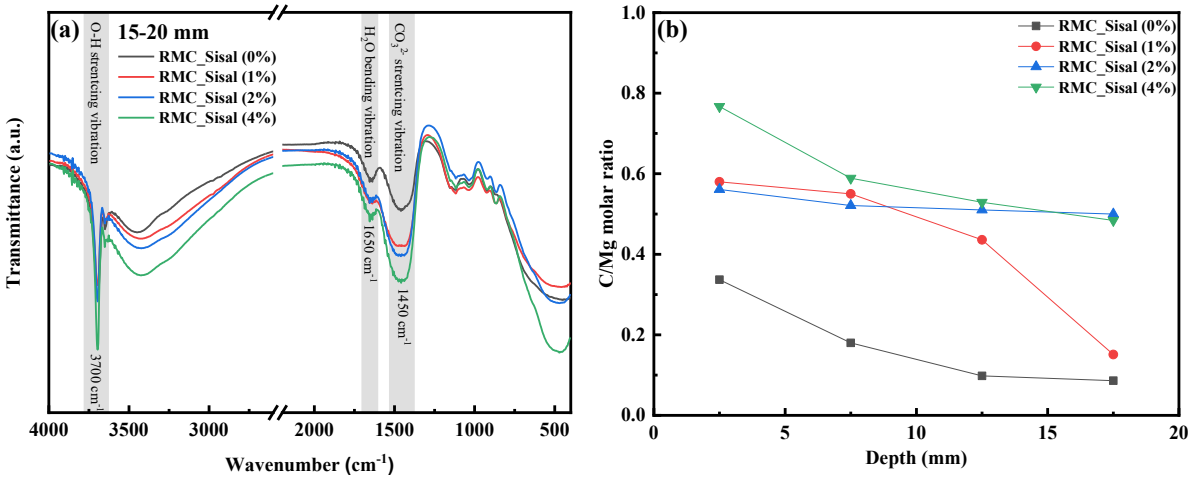

Fig. 4. (a) FTIR spectra of the RMC with different contents of sisal fiber at the depth of 15-20 mm; (b) C/Mg molar ratio at different depths obtained from XPS characterization.

Fig. 5 compares the CO_2 emission of RMC with different sisal fiber contents. It can be seen the CO_2 emission drops from about 37 kg/(m^3·MPa) of RMC_Sisal (0%) to 16 kg/(m^3·MPa) of RMC_Sisal (1%), which can be further reduced to 12.1 kg/(m^3·MPa) and 11.7 kg/(m^3·MPa) when the fiber content increase to 2 vol.% and 4 vol.%, respectively. The sustainability of RMC was frequently questioned due to its high CO_2 emission during production (e.g., 1.7 tonne/tonne of MgO vs. 1.1 tonne/tonne of PC [23]), low mechanical strength (e.g., 39.9 MPa of RMC vs. 59.9 MPa of PC [24, 25]), and low carbonation degree (e.g., below 0.2 [4, 11]). By adding minor sisal fiber and silica sand, the mechanical strength and carbonation degree can be enhanced prominently, this may alleviate concerns about the sustainability of RMC.

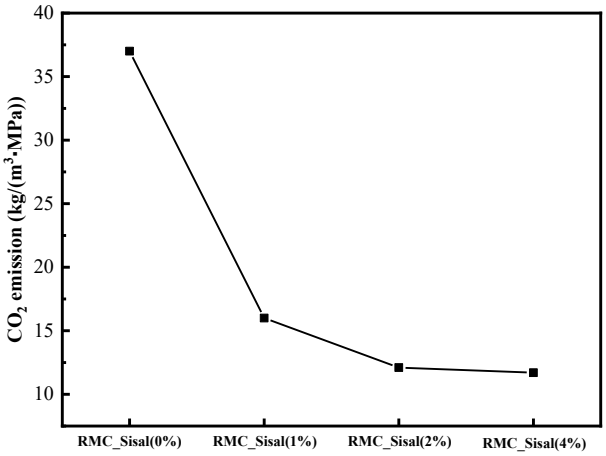

Fig. 5. CO_2 emission of RMC with different sisal fiber contents.

4 Conclusion

This work investigated the mechanical strength and carbonation degree of RMC incorporating silica sand and different contents of sisal fiber. The mechanical strength results suggested that the addition of minor sisal fiber (e.g., 2 vol.%) can significantly enhance the compressive strength to 92.6 MPa, which is about 2.2 times that of the control group; the RMC incorporating 4 vol.% sisal fiber demonstrated a strain-hardening behavior and comparable flexural strength to PC, the substitution of sisal fiber with PVA fiber improved the ductility but reduced the flexural strength. Carbonation depth in the control group was almost zero while it can continually increase to the maximum value (e.g., 20 mm) in the presence of 2 vol.% or more sisal fibers. XPS results directly proved that the carbonation degree in RMC with 2 vol.% or more sisal fibers was more than 3 times that of the control group. The increase in mechanical strength and carbonation degree leaded to a sharp reduction of CO_2 emission from 37 kg/(m^3·MPa) of the control group to 12 kg/(m^3·MPa) of RMC containing 2 vol.% sisal fiber. Accordingly, the addition of sisal fiber and silica sand can be a feasible approach to make RMC more sustainable and applicable.

References

[1] I. Chang, M. Lee, G.-C. Cho, Energies. **12**, 2567 (2019)

[2] H.-L. Wu, D. Zhang, B.R. Ellis, V.C. Li, Constr. Build. Mater. **191**, 23-31 (2018)

[3] J. Qiu, S. Ruan, C. Unluer, E.-H. Yang, Cement. Concrete. Res. **115**, 401-413 (2019)

[4] N. Dung, A. Lesimple, R. Hay, K. Celik, C. Cement. Concrete. Res. **125**, 105894 (2019)

[5] D. Zhang, H. Wu, V.C. Li, B.R. Ellis, Constr. Build. Mater. **238**, 117672 (2020)

[6] C. Xue, W. Li, Z. Luo, K. Wang, A. Castel, Cement. Concrete. Res. **139**, 106252 (2021)

[7] M.A. Sherir, K.M. Hossain, M. Lachemi, Constr. Build. Mater. **148**, 789-810 (2017)

[8] N. Dung, C. Unluer, Cement. Concrete. Comp. **82**, 152-164 (2017)

[9] N. Dung, C. Unluer, Cement. Concrete. Res. **118**, 92-101 (2019)

[10] N. Dung, C. Unluer, Constr. Build. Mater. **143**, 71-82 (2017)7.

[11] R. Hay, K. Celik, Cement. Concrete. Res. **128**, 105941 (2020)

[12] B. Wu, J. Qiu, J. CO_2. Util. **57**, 101874 (2022)

[13] N. Dung, C. Unluer, Cement. Concrete. Res. **103**, 160-169 (2018)

[14] I. Singh, R. Hay, K. Celik, Cement. Concrete. Res. **152**, 106673 (2022)

[15] J.H. Lee, J.H. Kim, Constr. Build. Mater. **341**, 127618 (2022)

[16] T. Zhang, X. Liang, C. Li, M. Lorin, Y. Li, L.J. Vandeperre, C.R. Cheeseman, Cement. Concrete. Res. **88**, 36-42 (2016)

[17] S. Ruan, J. Qiu, E.-H. Yang, C. Unluer, Cement. Concrete. Comp. **89**, 52-61 (2018)

[18] V. Anggraini, A. Asadi, A. Syamsir, B.B. Huat, Measurement. **111**, 158-166 (2017)

[19] S. Ruan, J. Qiu, E.-H. Yang, C. Unluer, Constr. Build. Mater. **269**, 121360 (2021)

[20] N. Dung, R. Hay, A. Lesimple, K. Celik, C. Unluer, Cement. Concrete. Comp. **115**, 103826 (2021)

[21] J. Wei, C. Meyer, Cement. Concrete. Res. **73**, 1-16 (2015)

[22] S. Li, Z.J. Wang, T.-T. Chang, PloS. One. **9**, e88648 (2014)

[23] D. Hassan, University of Cambridge, 2014.

[24] R. Zhang, D.K. Panesar, J. Clean. Prod. **271**, 122021 (2020)

[25] R. Zhang, A. Arrigoni, D.K. Panesar, C Cement. Concrete. Comp. **124**, 104263 (2021)